INVESTIGATION AND REDUCTION OF RADIATION HEAT LOSSES FROM A ROTARY KILN BY USING LOW-EMISSIVITY PAINT

Habib Ullah Khan[1]*, Muhammad Alamzeb Khan[1], Wilayat Said[1], Seemab Zahid[1], Syed Muhammad Arifain[1]

[1] Department of Mechanical Engineering, University of Engineering and Technology Peshawar, Peshawar, Pakistan

* **Corresponding author:** Habib Ullah Khan
Email: khanh9902@gmail.com

Abstract

Rotary kilns are thermal processing units used for processing solid materials at extremely high temperatures. In the cement industry, calcination takes place inside a rotary kiln and is a highly energy-intensive process. This paper investigates the reduction of radiative heat loss from the kiln surface by applying a low-emissivity coating and simulates the physical behavior inside the kiln using ANSYS. The study also considers the need for a practical emissivity value because decreasing surface emissivity reduces radiative heat loss but increases kiln-shell temperature. A detailed heat-transfer analysis was conducted to quantify the effect of surface emissivity on shell temperature. For the baseline case, the total surface heat loss was approximately 5.17 MW, with about 70% due to radiation and 30% due to convection. The analysis suggests an emissivity of 0.6, for which the shell temperature increases by approximately 45 °C while the total heat loss decreases by approximately 250 kW (4.8%). Using a net calorific value of 25.958 MJ/kg, this corresponds to an estimated coal saving of approximately 832 kg/day. The results indicate that a low-emissivity coating can reduce kiln heat loss, although the accompanying increase in shell temperature must also be considered.

Keywords: rotary kiln, radiation, convection, emissivity, low-emissivity coating, ANSYS Fluent, heat loss

1. Introduction

Rotary kilns are advanced thermal-processing units that are used by various industries to process solid materials at high temperatures. In the cement industry, calcination and clinker formation take place inside the rotary kiln and require high thermal energy input [1], [2]. Because of the high internal temperature, the external kiln shell can reach several hundred degrees Celsius and lose a considerable amount of heat through convection and thermal radiation. Recent industrial studies also identify convection and radiation from the kiln shell as an important part of the recoverable heat loss from cement kilns [3].

For complete analysis of a rotary kiln, the internal wall and gas-temperature profiles are needed. Direct measurement inside an operating kiln is difficult because of the high temperature, sealed environment and continuous rotation [4]. In order to estimate the internal temperature profile of the wall and combustion gases, a computational fluid dynamics (CFD) model was used. CFD allows the gas and wall temperatures to be estimated for the fuel and air-flow conditions used in the industrial case. The results from the CFD analysis were then used together with external heat-transfer calculations to estimate heat loss to the atmosphere.

Emissivity is a surface radiative property that describes how efficiently a surface emits thermal radiation. The emissivity of a surface depends on wavelength, direction and surface condition [5]. In this study the kiln shell is treated as a diffuse surface, and a representative total surface emissivity is used in the heat-transfer calculations.

Radiation-barrier coatings, or low-emissivity coatings, are formulated to reduce radiative heat transfer by reducing the surface emissivity. Such coatings commonly use a polymer or silicone-based binder with metallic pigments such as aluminum. Their performance depends on the binder-to-pigment ratio, temperature and oxidation behavior. Previous work on polysiloxane/aluminum coatings showed that suitable formulations can retain low infrared emissivity at elevated temperatures and that a pigment-to-binder ratio of 1.0 can maintain coating integrity up to about 600 °C [6].

The emissivity of a surface also depends on its fabrication, thermal history and interaction with the environment [5]. Since rotary-kiln shells are generally steel surfaces exposed to high temperatures and oxidation, an initial external-surface emissivity of 0.9 was used in the baseline calculations to represent a dark, heavily oxidized surface.

ANSYS Fluent uses the finite-volume method, in which the computational domain is discretized into a finite number of control volumes [7]. The present analysis uses geometric and operating data collected from an industrial cement rotary kiln during the original project.

2. Methodology

In this study, a method was developed to reduce radiation heat loss from the kiln surface by applying a low-emissivity coating. Decreasing surface emissivity reduces radiative heat loss [6], but it also increases kiln-shell temperature. The effect of emissivity on shell temperature must therefore be evaluated before selecting a coating, since higher shell temperatures can increase thermal loading in the shell and refractory system [8]. The main steps of the study are shown in Figure 1.

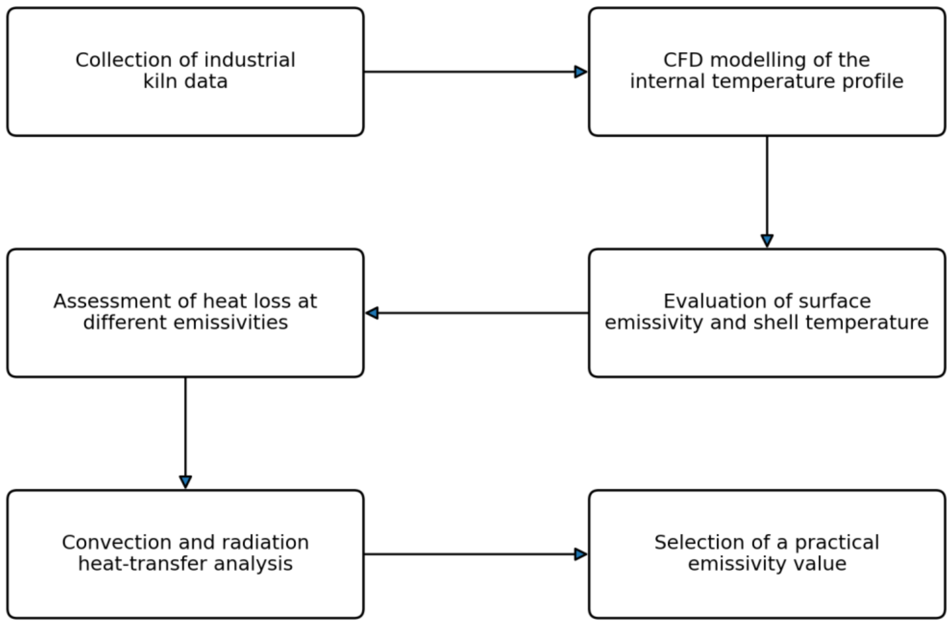

Figure 1. Main steps used to assess the effect of a low-emissivity coating on rotary-kiln heat loss.

To model the rotary kiln in ANSYS CFD, the following assumptions were made:

- The kiln was represented as a simplified cylindrical structure.
- Steady-state conditions were assumed.
- The effect of gravity was neglected.
- The gas flow was treated as incompressible.

The geometry was created in ANSYS SpaceClaim using the kiln dimensions from the industrial case study. Primary air enters the kiln through concentric passages around the fuel inlet, and the burner tip is located 1 m inside the kiln. The secondary-air inlet is located at the start of the rotary kiln.

Table 1. Kiln geometry and burner specifications used in the industrial case study.

Parameter	Value	Unit
Kiln length	52,000	mm
Inner diameter	4,000	mm
Outer diameter	4,400	mm
Burner type	Sino flame full-power coal burner	
Diameter of axial-air inlet	395	mm

Diameter of fuel inlet	355	mm
Diameter of swirl-flow inlet	450	mm
Diameter of secondary-air inlet	4,000	mm
Diameter of outlet	4,000	mm

Meshing is the discretization of the geometry into smaller elements or control volumes where the governing equations are solved. A finer mesh can improve spatial resolution but increases computational cost [7]. The mesh was therefore refined near the burner tip and combustion zone, where larger flow and temperature gradients were expected, and made coarser farther from the burner. A separate mesh-independence analysis was not included in the original study.

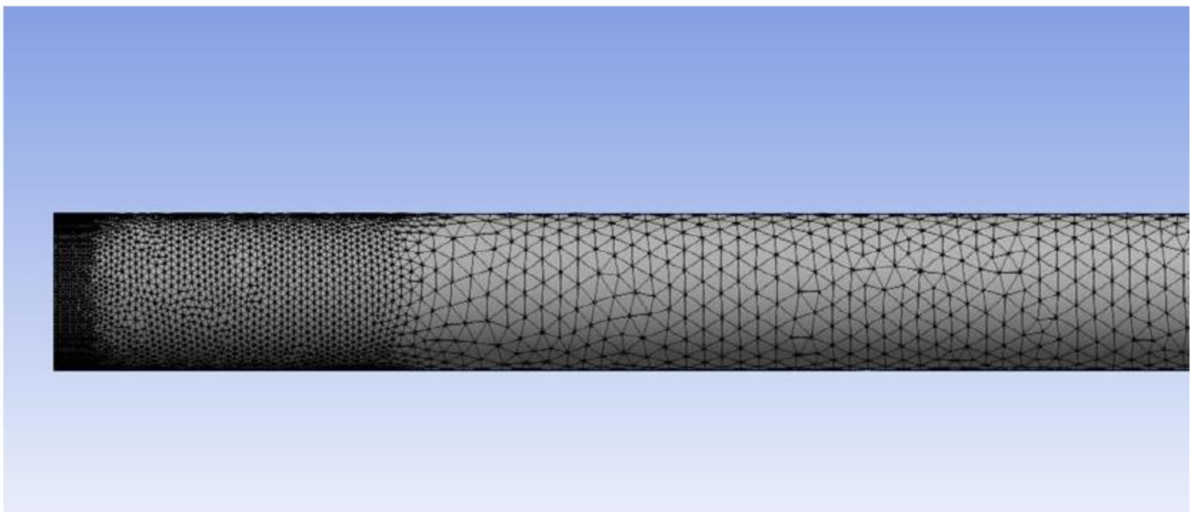

Figure 2. Computational mesh, refined near the burner region and coarser farther along the kiln.

A pressure-based solver was used in ANSYS Fluent under the assumption of incompressible flow [7], [9]. The energy equation was enabled, and the RNG k-ε model was used to represent turbulent flow inside the kiln. This model was selected as a modified form of the standard k-ε turbulence model suitable for the turbulent conditions considered in the original analysis.

Radiative heat transfer was modeled using the P-1 radiation model. The P-1 model is commonly used for participating-media radiation in combustion calculations and has also been applied in full-scale rotary-cement-kiln CFD studies [10]. Radiation modeling was required because radiative transfer strongly affects the temperature distribution in the kiln.

Fuel combustion was represented using a non-premixed species model because the fuel and combustion air enter the kiln separately. Sub-bituminous coal properties were defined from the available coal composition, and the required mixture and enthalpy information was generated for the simulation. The inlets were defined as mass-flow inlets and the kiln exit as a pressure outlet. The air-to-fuel ratio used in the case study was 9.3 and increased to 10.59 kg of air per kg of coal with the excess-air condition used in the model. Primary air represented 10% of the total air supply and secondary air 90%.

Table 2. Boundary conditions used in the CFD model.

Boundary	Mass flow rate (kg/s)	Temperature (K)
Total air	10.59	
Fuel	1.000	300
Axial air	0.1059	300

Cooling air	0.1059	300
Swirl air	0.8472	300
Secondary air	9.531	1050

The solution was initialized using hybrid initialization. The first 250 iterations were performed using first-order spatial discretization to obtain a stable solution, followed by 50 iterations using second-order spatial discretization.

2.1 External convection from the kiln shell

To calculate convection heat loss from the kiln shell, the external convection coefficient was first evaluated. Natural, forced and mixed convection were considered. When a higher-velocity air stream flows over the kiln surface, forced convection becomes more important. For cross-flow over a cylinder, the average forced-convection Nusselt number was calculated using the Churchill-Bernstein correlation [5]:

$$\overline{Nu}_F = 0.3 + \frac{0.62 Re_D^{1/2} Pr^{1/3}}{\left[1 + (0.4/Pr)^{2/3}\right]^{1/4}} \left[1 + \left(\frac{Re_D}{282000}\right)^{5/8}\right]^{4/5}$$

Table 3. Parameters used for the forced-convection calculation.

Quantity	Symbol	Value	Unit
Thermal conductivity	k	0.0368	W/m·K
Outer kiln diameter	D	4.4	m
Air velocity	V	4.5	m/s
Kinematic viscosity	ν	31.55×10^{-6}	m^2/s
Reynolds number	Re_D	627,416	-
Prandtl number	Pr	0.6865	-
Forced Nusselt number	Nu_F	827.58	-
Forced-convection coefficient	h_F	6.9	$W/m^2 \cdot K$

Natural convection becomes important when the external air velocity is low. In free convection, the Nusselt number depends on the Rayleigh and Prandtl numbers, while the Grashof number represents the relative importance of buoyancy and viscous effects [5]. The values used for the natural-convection calculation are summarized in Table 4.

Table 4. Parameters used for the natural-convection calculation.

Quantity	Symbol	Value	Unit
Thermal conductivity	k	0.0368	W/m·K
Outer kiln diameter	D	4.4	m
Kinematic viscosity	ν	31.55×10^{-6}	m^2/s
Rayleigh number	Ra_D	3.38×10^{11}	-
Prandtl number	Pr	0.6865	-
Natural Nusselt number	Nu_N	863.3	-
Grashof number	Gr	4.92×10^{11}	-
Thermal expansion coefficient	β	0.002257	K^{-1}
Natural-convection coefficient	h_N	7.22	$W/m^2 \cdot K$
Surface temperature	T_s	300	°C
Ambient temperature	T_∞	40	°C

The relative contribution of natural and forced convection can be assessed using the ratio Gr/Re^2. In the transition region, both mechanisms contribute and a mixed-convection model is more appropriate. The mixed Nusselt number was estimated from [5]:

$$Nu^n = Nu_F^n + Nu_N^n, \qquad n = 4$$

For transverse flow over the cylinder, n = 4 was used. Combining the forced and natural terms gives a mixed-convection coefficient of approximately 8.4 W/m²·K for the baseline condition.

2.2 Assessment of heat loss from the rotary kiln

After estimating the external heat-transfer parameters, convection and radiation losses from the kiln surface were calculated. Convection heat loss was obtained from Newton's law of cooling [5]. Table 5 summarizes the baseline parameters.

Table 5. Parameters for convection heat loss from the kiln surface.

Quantity	Value	Unit
Outer diameter	4.4	m
Length	52	m
Mixed convection coefficient, h	8.4	W/m²·K
Surface temperature, T_s	300	°C
Ambient temperature, T_∞	40	°C
Convection heat loss, q_conv	1,569	kW

Radiation heat loss from the kiln surface was calculated using the standard two-surface radiation relation [5]. The external shell was treated as a heavily oxidized steel surface with an emissivity of 0.9. The baseline radiation calculation is summarized in Table 6.

Table 6. Parameters for radiation heat loss from the kiln surface.

Quantity	Value	Unit
View factor	1	-
Surface emissivity, ε	0.9	-
External surface area, A	718.4	m²
Stefan-Boltzmann constant, σ	5.67×10^{-8}	W/m²·K⁴
Surface temperature, T_s	300 (573)	°C (K)
Ambient temperature, T_∞	40 (313)	°C (K)
Radiation heat loss, q_rad	3,600	kW

The total surface heat loss was taken as the sum of convection and radiation losses:

$$q_{tot} = q_{conv} + q_{rad}$$

To evaluate how the shell temperature changes with emissivity, an ANSYS steady-state thermal model was also used. The inner kiln-surface temperature was set to 1800 °C, while the wall thermal properties, external convection coefficient and ambient temperature were applied as boundary conditions. Surface emissivity was varied in increments of 0.05 and the resulting outer-shell temperature was recorded. In this analysis, the thermal resistance of the kiln wall was assumed to remain unchanged after application of the coating so that the effect of surface emissivity could be evaluated independently.

3. Results

3.1 CFD temperature field

Based on the model and boundary conditions, the combustion analysis was performed in ANSYS Fluent. The temperature contours were displayed on a plane passing through the middle of the kiln. Figure 3 shows the gas-temperature distribution along the kiln length.

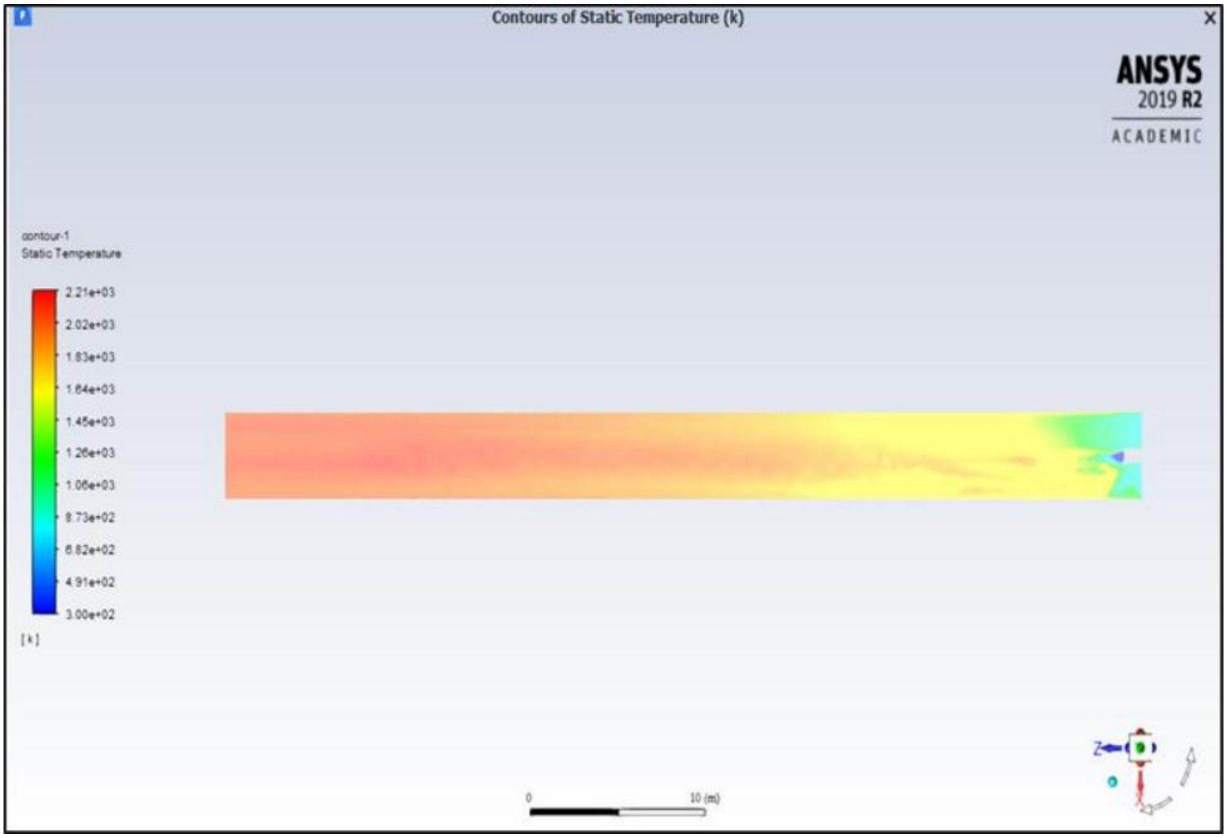

Figure 3. Gas-temperature contour along the length of the kiln.

To examine the internal wall temperature, a line was defined along the kiln wall and the temperature profile was extracted. A second line was defined through the gas region to obtain the gas-temperature profile. The resulting wall and gas-temperature trends, together with the bed-temperature curve from the original analysis, are shown in Figure 4.

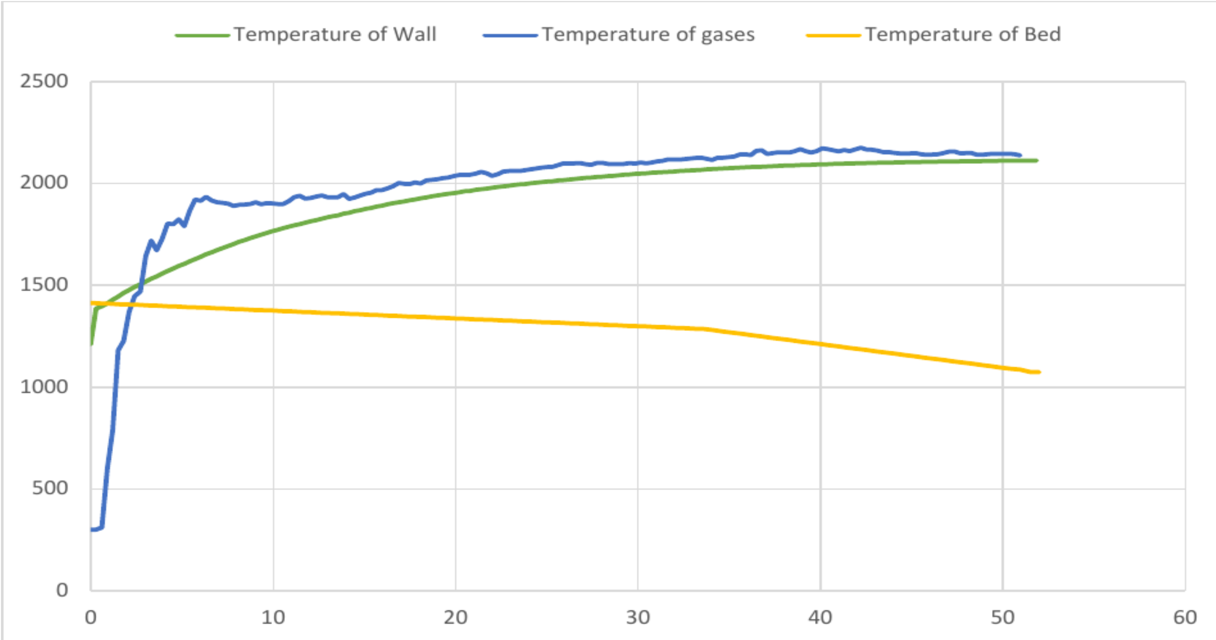

Figure 4. Wall, gas and bed-temperature profiles at a fuel flow rate of 1 kg/s.

The wall temperature remains below the corresponding gas temperature over most of the kiln length. The gas temperature is relatively low near the burner tip because combustion is developing and then rises along the kiln before reaching a high-temperature region. Direct internal temperature measurements were not available for this case study. The predicted ranges were therefore compared with published rotary-kiln CFD studies and the operating-zone temperature ranges available during the original project [1], [10], [11]. This should be considered a consistency comparison rather than a full experimental validation.

3.2 External convection and radiation

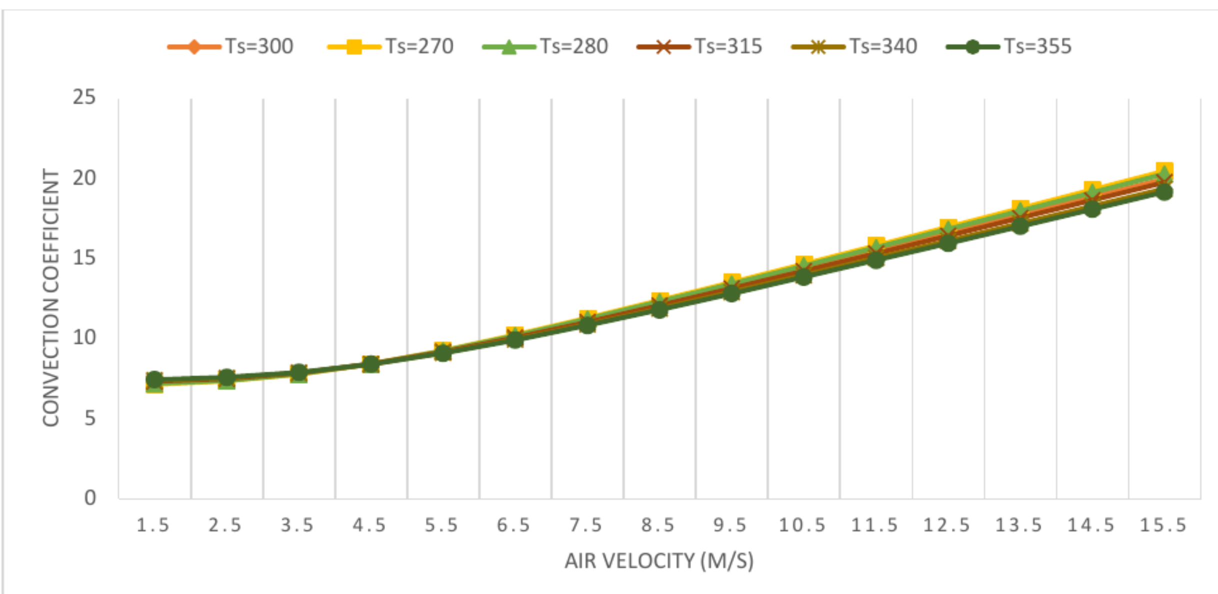

Figure 5. Mixed-convection coefficient at different air velocities and surface temperatures.

Figure 5 shows the variation of the mixed-convection coefficient with air velocity. At lower air velocities, natural convection has a stronger influence, while forced convection becomes increasingly important as air velocity rises. Around the 4-5 m/s range used in the baseline case, both mechanisms contribute and the mixed-convection model is appropriate.

Radiation heat loss depends directly on the surface emissivity. At a fixed surface temperature, reducing emissivity decreases the radiative component of the heat loss, as shown in Figure 6.

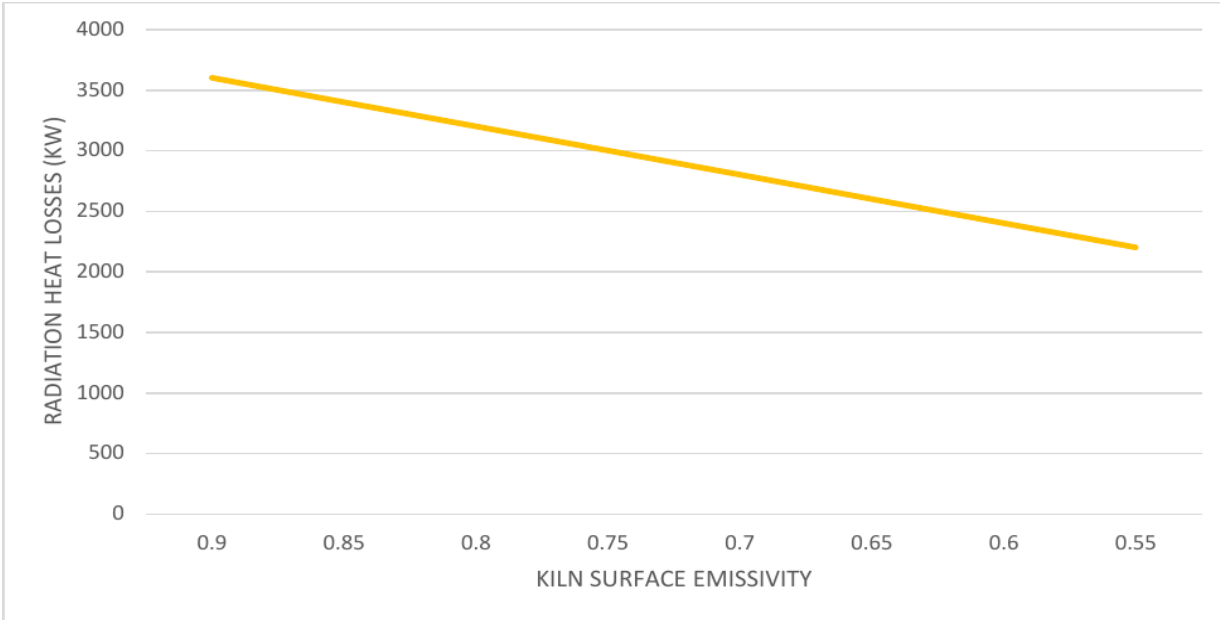

Figure 6. Radiation heat loss as surface emissivity decreases for the baseline shell temperature.

3.3 Total heat loss and effect of surface temperature

For the 52 m long, 4.4 m external-diameter kiln at a baseline shell temperature of 300 °C and emissivity of 0.9, the calculated heat loss was approximately 5.17 MW. About 1.57 MW was due to convection and 3.60 MW to radiation, corresponding to approximately 30% convection and 70% radiation. This distribution is also consistent with recent kiln-shell heat-loss studies in which radiation was reported as the larger component of the combined radiation-convection loss [3].

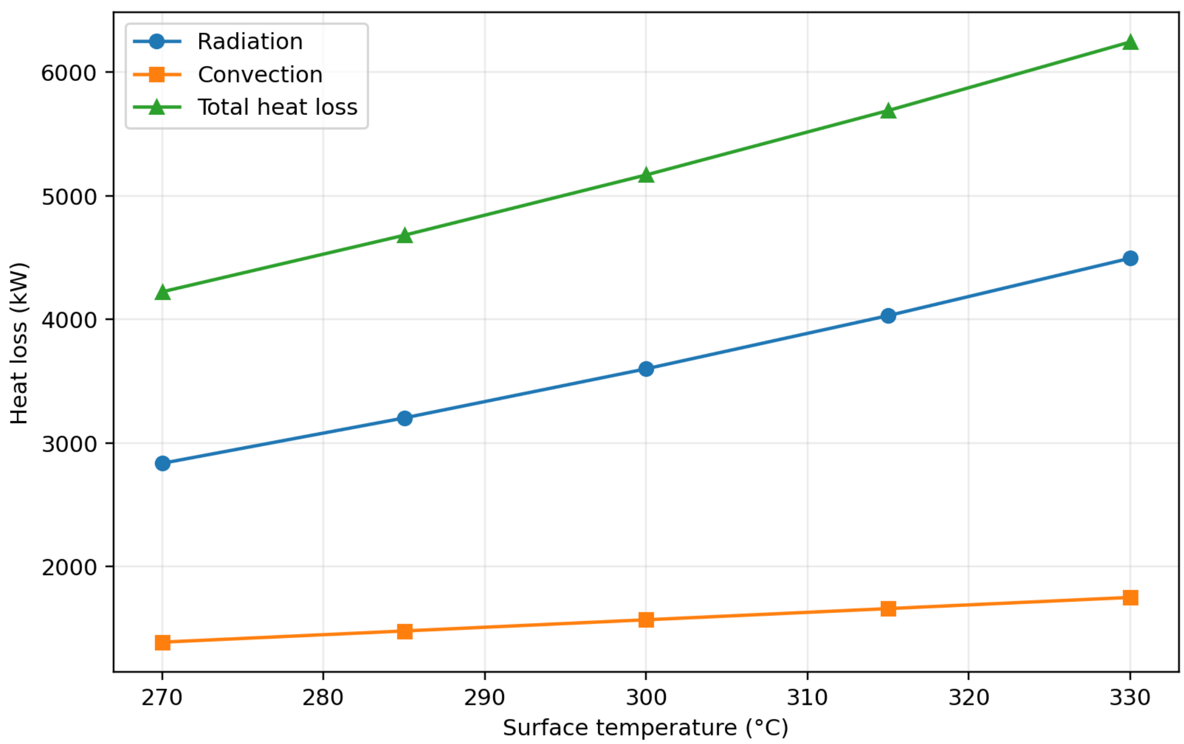

Figure 7. Calculated radiation, convection and total heat loss at different kiln-shell temperatures.

The calculated heat loss increases as the shell temperature rises. Taking the 300 °C case as the reference, the recalculated values are shown in Table 7.

Table 7. Calculated total heat loss at different shell temperatures relative to the 300 °C baseline.

Surface temperature (°C)	Total heat loss (kW)	Change relative to 300 °C
270	4,223	-18.3%
285	4,681	-9.4%
300	5,169	Reference
315	5,690	+10.1%
330	6,245	+20.8%

3.4 Effect of emissivity on shell temperature

The steady-state thermal analysis shows that the external shell temperature increases as surface emissivity decreases. In the original project, an increase of approximately 50 °C above the baseline shell temperature was used as the operating constraint for selecting a practical emissivity value. Figure 8 shows the predicted trend.

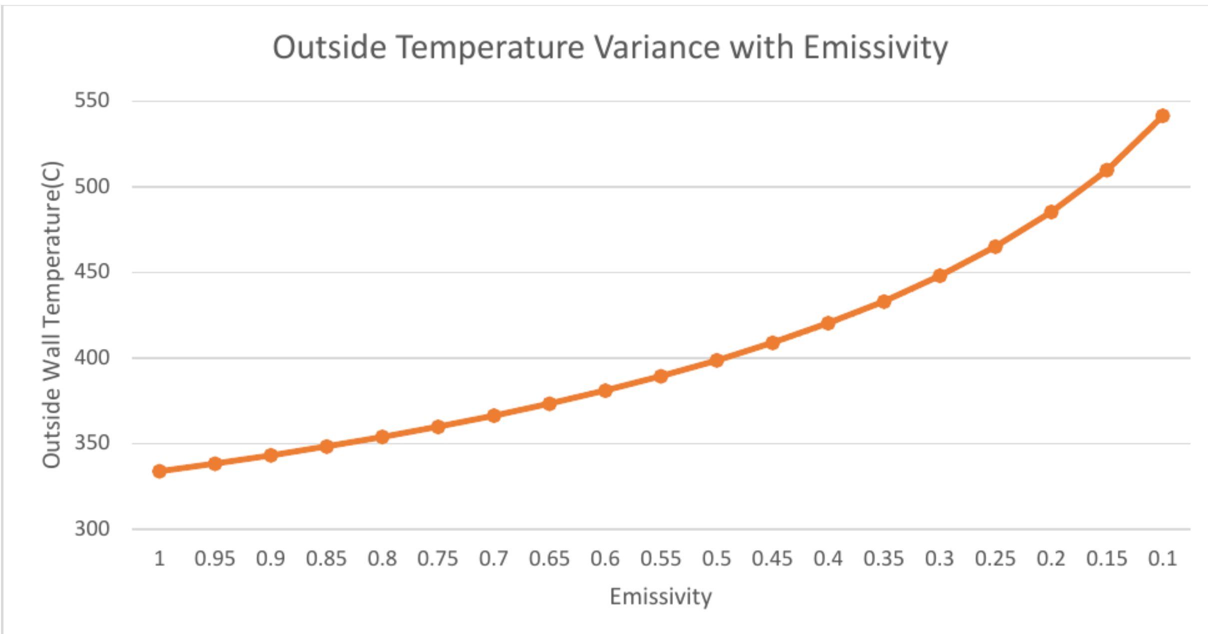

Figure 8. Predicted increase in outside wall temperature as surface emissivity decreases.

Based on this project constraint, an emissivity of 0.6 was selected. The predicted shell temperature increases by approximately 45 °C, while the total heat loss decreases from about 5.17 MW to about 4.92 MW. The resulting energy saving is approximately 250 kW, or 4.8% of the baseline surface heat loss. Using the plant-fuel net calorific value reported in the original calculations (25.958 MJ/kg), the corresponding estimated reduction in coal use is approximately 832 kg/day.

4. Discussion

A substantial amount of energy is lost through radiation and convection from the rotary-kiln shell. The cement industry is highly energy intensive, and the kiln is one of the main thermal-processing units. The proposed method uses a low-emissivity coating to reduce the radiative component of the shell heat loss. The approach is relatively simple in concept because it changes the surface radiative property rather than modifying the main kiln process.

There is also a concern that must be addressed before lowering the emissivity. Blocking part of the radiative heat loss increases the shell temperature. Higher shell temperatures and thermal gradients can increase thermal and mechanical loading in rotary-kiln shells and refractory systems [8]. For this reason, the coating should not be selected only on the basis of the maximum possible heat-loss reduction.

For the baseline case, the mixed-convection and radiation calculations give a total shell heat loss of approximately 5.17 MW. Radiation is the larger component, so reducing emissivity has a noticeable effect on total heat loss. An emissivity of 0.6 provides an estimated saving of approximately 250 kW while keeping the predicted shell-temperature increase within the operating constraint used in the original project. The corresponding fuel saving is approximately 832 kg/day based on the reported net calorific value. A reduction in fuel consumption would also reduce the combustion-related emissions associated with the saved coal. A specific annual CO_2 value is not reported because emissions were not independently quantified in this study.

The selected emissivity value should be treated as a case-study result rather than a universal limit for all cement kilns. Actual coating performance depends on the coating composition, oxidation, surface condition and long-term exposure to high temperatures [6]. Likewise, acceptable shell-temperature limits depend on the kiln design, refractory condition and operating practice.

4.1 Limitations

The study has several limitations. The kiln was represented using simplified geometry and steady-state operating conditions, and gravity was neglected in the CFD model. Direct measurements of the internal gas and wall temperatures were not available for quantitative validation. The coating was modeled mainly through its effect on surface emissivity, while long-term effects such as coating degradation, oxidation and changes in surface condition were not modeled. The predicted 250 kW saving should therefore be interpreted as a model-based estimate for the conditions considered rather than a direct plant measurement.

5. Conclusion

For the kiln geometry considered in this study (external diameter 4.4 m and length 52 m) at an average external shell temperature of 300 °C, the calculated total surface heat loss is approximately 5.17 MW. About 30% of this loss is associated with convection and 70% with thermal radiation. The relative importance of natural and forced convection changes with external air velocity, and a mixed-convection model is appropriate around the baseline 4-5 m/s condition.

Reducing the shell emissivity decreases radiation heat loss but increases the external shell temperature. Based on the operating constraint used in the original project, a coating emissivity of 0.6 gives a suitable balance between these two effects. At this emissivity, the predicted total heat loss decreases to approximately 4.92 MW, giving an energy saving of about 250 kW, while the shell temperature increases by approximately 45 °C.

The results indicate that low-emissivity coatings can reduce heat loss from rotary kilns. However, the increase in shell temperature and the thermal response of the shell and refractory system should be considered before practical implementation. Experimental evaluation under operating kiln conditions would be useful for confirming the predicted energy saving and the long-term performance of the coating.

Acknowledgments

The authors acknowledge the support received during the original BSc research project at the University of Engineering and Technology (UET) Peshawar and the industrial personnel who provided kiln operating data and technical information for the case study.

Author Contributions

Habib Ullah Khan: Conceptualization, methodology, CFD modelling and simulation, formal analysis, visualization, and writing of the original draft. Muhammad Alamzeb Khan: Supervision, methodology, project guidance, and review and editing. Wilayat Said, Seemab Zahid, and Syed Muhammad Arifain: Project collaboration, data collection, literature review, analysis support, and review of the manuscript. All authors reviewed and approved the final manuscript.

Declaration of Generative AI Use

Generative AI tools were used during manuscript preparation to assist with language editing, formatting and clarity. They were not used to generate or alter the underlying simulation data, calculations or results. The authors reviewed and verified the final manuscript and take responsibility for its content.

Competing Interests

The authors declare no known competing interests related to this work.

References

[1] W. K. H. Ariyaratne, A. Malagalage, M. C. Melaaen, and L.-A. Tokheim, "CFD modelling of meat and bone meal combustion in a cement rotary kiln – Investigation of fuel particle size and fuel feeding position impacts," *Chem. Eng. Sci.*, vol. 123, pp. 596–608, Feb. 2015, doi: 10.1016/j.ces.2014.10.048.

[2] FEECO International, Inc., "The FEECO Rotary Kiln Handbook," FEECO International, Inc.

[3] B. T. Tola and L. F. Wako, "Design and analysis of waste heat recovery heat exchanger from external kiln shell in cement plant," *Int. J. Thermofluids*, vol. 33, p. 101623, May 2026, doi: 10.1016/j.ijft.2026.101623.

[4] H. Xu, Q. Hou, X. Chen, W. Wang, and T. Shen, "A soft sensing approach driven by data and model for estimating internal temperature and refractory lining thickness in rotary kilns," *Measurement*, vol. 275, p. 121405, May 2026, doi: 10.1016/j.measurement.2026.121405.

[5] T. L. Bergman, A. S. Lavine, F. P. Incropera, and D. P. DeWitt, *Fundamentals of Heat and Mass Transfer*, 8th ed. Wiley, 2017.

[6] J. Zhao *et al.*, "The High-Temperature Resistance Properties of Polysiloxane/Al Coatings with Low Infrared Emissivity," *Coatings*, vol. 8, no. 4, p. 125, Mar. 2018, doi: 10.3390/coatings8040125.

[7] ANSYS, Inc., "ANSYS Fluent Theory Guide," ANSYS, Inc., Canonsburg, PA, USA, User/Technical Manual Release 2019 R2.

[8] W. D. Guillin-Estrada *et al.*, "Transient operation effects on the thermal and mechanical response of a large-scale rotary kiln," *Results Eng.*, vol. 14, p. 100396, Jun. 2022, doi: 10.1016/j.rineng.2022.100396.

[9] H. F. M. Elattar, "Flame simulation in rotary kilns using computational fluid dynamics," Ph.D. dissertation, Otto-von-Guericke University Magdeburg, Magdeburg, 2011. doi: 10.25673/5349.

[10] D. Lahaye, F. Juretić, and M. Talice, "Modelling a Turbulent Non-Premixed Combustion in a Full-Scale Rotary Cement Kiln Using reactingFoam," *Energies*, vol. 15, no. 24, p. 9618, Dec. 2022, doi: 10.3390/en15249618.

[11] S. Wang, J. Lu, W. Li, J. Li, and Z. Hu, "Modeling of Pulverized Coal Combustion in Cement Rotary Kiln," *Energy Fuels*, vol. 20, no. 6, pp. 2350–2356, Nov. 2006, doi: 10.1021/ef060027p.